Langmuir

ARTICLE

pubs.acs.org/Langmuir

Membrane Morphology Modifications Induced by Hydroquinones

Sérgio S. Funari,*,† Vivian Rebbin,† Liliana Marzorati,‡ and Claudio di Vitta*,‡

†HASYLAB/Deutsches Elektronensynchrotron (DESY), Notkestrasse 85, 22607 Hamburg, Germany

‡Institute of Chemistry, University of Sao Paulo, 05508-900 Sao Paulo, Brazil

ABSTRACT: We synthesize and characterize alkylthiohydroquinones (ATHs) in order to investigate their interactions with lipid model membranes, POPE and POPC. We observe the formation of structures with different morphologies, or curvature of the lipid bilayer, depending on pH and increasing temperature. We attribute their formation to changes in the balance charge/polarity induced by the ATHs. Mixtures of ATHs with POPE at pH 4 form two cubic phases, $P4_332$ and $Im3m$, that reach a maximum lattice size at 40 °C while under basic conditions these phases only expand upon heating from room temperature. The cubic phases coexist with lamellar or hexagonal phases and are associated with inhomogeneous distribution of the ATH molecules over the lipid matrix. The zwitterionic POPC does not form cubic phases but instead shows lamellar structures with no clear influence of the 2,6-BATH.

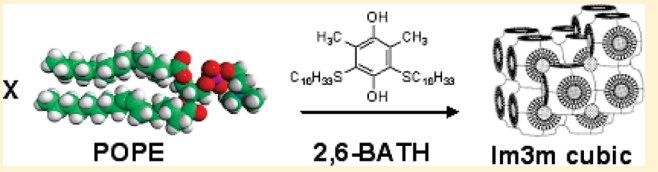

INTRODUCTION

Quinones are natural or synthetic molecules, taking part in a wide range of processes in organisms. Among them, two important groups of lipid-soluble benzoquinones are plastoquinones (**1**, Pqs; Scheme 1) and ubiquinones (**2**, Coenzymes Q-CoQs; Scheme 1). These benzoquinones are structurally analogous and are both involved in the electron transport chain in eukariotic cells. The naturally occurring members of plastoquinones and ubiquinones have $n = 9$ and $n = 6-10$ *trans*-isoprenoid side chains, respectively, with Pq, having $n = 9$, being found in chloroplasts, while CoQ with $n = 10$ is found in the inner membrane of human mitochondria. Both Pqs and CoQs interact with NADH, being reduced to the corresponding hydroquinones.[1]

Several quinones are used as antitumor and anti-infection agents. For example, doxorubicin is used as a frontline chemotherapeutic agent, whereas certain naphthoquinones like diospyrin and methyljuglone are particularly effective against *Mycobacterium tuberculosis*. Alkylthiobenzoquinones can show toxicological activity, e.g., 2,6-dichloro-3-(glutathion-*S*-yl)-1,4-benzoquinone showed a 41-fold increase in the rate of GSH-transferase inhibition when compared with the parent quinone. Dodecylthioxyloquinone and similar xyloquinones inhibit coenzyme Q in mitochondrial succinoxidase and NADH oxidase systems. 5-Pentadecenylresorcinols (a phenolic compound, like hydroquinones) isolated from *Ginkgo biloba* presents strong activity against S180 tumor in mice.[2]

We synthesized new ATHs (Scheme 2), in order to investigate different aspects of lipid-soluble hydroquinones interactions with phospholipids normally found in cell membranes.

2,5-ATH and 2,6-BATH have the same long hydrophobic alkyl chains found in many lipids forming the cell membranes. In these compounds, the tails should share the inner core of the membrane, while the hydroquinone, as a polar headgroup, should remain on the surface. One or more alkylthio chains attached to the aromatic ring modifies its hydrophobicity and should alter the electron distribution. Moreover, the two OH groups become chemically distinguishable, e.g., by NMR spectroscopy, and also show different pK_a values.

Lipids have been extensively studied in the last decades and the structure of their self-assembled domains characterized.[3] A wealth of information is available in the literature concerning the thermal phase transitions occurring in these systems[4−6] and also about the influence of other components,[7] such as additives[8] and ionic strength of the environment.[9] Moreover, theoretical models dealing with bilayer stability[10] and structural aspects of phase transitions have been proposed and are continuously being revised.[11,12]

EXPERIMENTAL SECTION

Synthesis of 2,5-ATH. A solution of 1.90 g (7.30 mmol) of *n*-hexadecanethiol in hexane (100 mL) was slowly added to a well-stirred solution of 1.00 g (7.30 mmol) of 2,5-dimethylbenzoquinone in ethanol (100 mL). After 2 h, the solvent was removed under reduced pressure and the residue was dissolved in dry acetone (70 mL). To this, a saturated solution of iron(III) nitrate (7.5 g, 31 mmol) was slowly added. 2,5-Dimethyl-3-hexadecylthiobenzoquinone was obtained, as a red solid (2.56 g, 6.53 mmol, 89%), after filtration and recrystallization from acetone: mp 70−72 °C; δ_H (300 MHz; $CDCl_3$) 0.83 (3H, t, $J = 6.6$ Hz), 1.18−1.65 (28H, m), 2.12 (3H, s), 2.40 (3H, s), 3.05 (2H, t, $J = 7.3$ Hz), 6.60 (1H, s). Anal. Calcd for $C_{24}H_{40}O_2S$ (%): H, 10.3; C, 73.4. Found: H, 10.6; C, 73.0. To a suspension of 1.3 g (3.3 mmol) of the above obtained red solid in a mixture of water (10 mL) and acetic acid (10 mL) was added excess of zinc (dust), until complete fading of the red color. After addition of water (50 mL), extraction with dichloromethane, neutralization of the organic phase with sodium bicarbonate, drying with

Received: December 10, 2010
Revised: May 9, 2011
Published: June 01, 2011

Scheme 1. General Formula of Two Groups of Lipid Soluble Benzoquinones: (1) Plastoquinones and (2) Ubiquinones

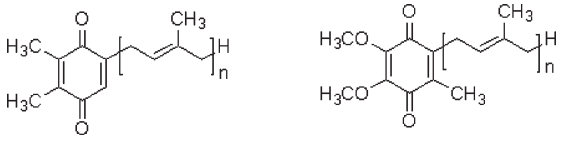

1 2

Scheme 2. Synthesis of 2,6-BATH [2,6-Bis(hexadecylthio)-3,5-dimethylbenzene-1,4-diol] and 2,5-ATH (2-Hexadecylthio-3,5-dimethylbenzene-1,4-diol)

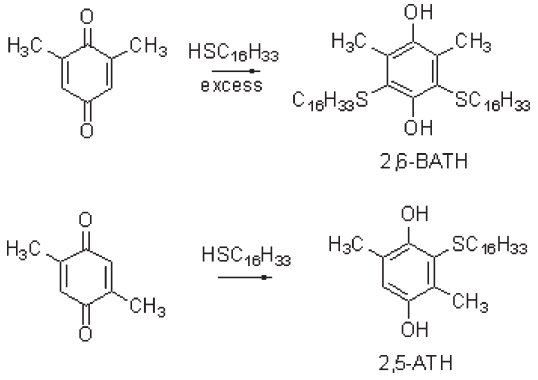

magnesium sulfate, and concentration, 0.73 g (1.8 mmol, 56%) of 2,5-ATH was obtained as a white solid: mp 74−78 °C; δ_H (300 MHz; $CDCl_3$) 0.88 (3H, bt), 1.18−1.65 (28H, m), 2.25 (3H, bs), 2.41 (3H, bs), 2.57 (2H, bt), 4.31 (1H, bs), 6.65 (1H, bs), 6.85 (1H, bs). Anal. Calcd for $C_{24}H_{42}O_2S$ (%): H, 10.7; C, 73.0. Found: H, 10.2; C, 73.5.

Synthesis of 2,6-BATH. A solution of 2.53 g (9.81 mmol) of *n*-hexadecanethiol in hexane (100 mL) was added to a well-stirred solution of 0.89 g (6.5 mmol) of 2,6-dimethylbenzoquinone in ethanol (100 mL). After 2 h, the solvent was removed under reduced pressure and the residue was dissolved in dry acetone (50 mL). To this, a saturated solution of iron(III) nitrate (6.3 g, 26 mmol) was slowly added. The first crop of crystals (0.80 g, 1.2 mmol, 19%) was collected, and after two recrystallizations from acetone, 2,6-dimethyl-3,5-di-*n*-hexadecylthiobenzoquinone, a pure red solid, was obtained: mp 48−51 °C; δ_H (300 MHz; $CDCl_3$) 0.88 (6H, t), 1.10−1.72 (56H, m), 2.23 (6H, bs), 3.05 (4H, t, J = 7.5 Hz). Anal. Calcd for $C_{40}H_{72}O_2S_2$ (%): H, 11.2; C, 74.0. Found: H, 10.8; C, 73.7. The red solid (0.70 g, 1.1 mmol) was dissolved in water (10 mL) and acetic acid (10 mL) and was treated with zinc (dust) until color fading. After addition of water (50 mL), extraction with dichloromethane, neutralization of the organic phase with sodium bicarbonate, drying with magnesium sulfate, and concentration, 0.62 g (0.95 mmol, 87%) of 2,6-BATH, as a white solid, was obtained: mp 60−62 °C; δ_H (300 MHz; $CDCl_3$) 0.85 (6H, t), 1.05−1.65 (56H, m), 2.45 (6H, bs), 2.67 (4H, t). Anal. Calcd for $C_{40}H_{74}O_2S_2$ (%): H, 11.5; C, 73.8. Found: H, 11.0; C, 73.4.

Sample Preparation. Preweighted amounts of the lipids (Avanti Polar Lipids, Inc., Alabaster, AL) POPE (1-palmitoyl-2-oleoyl-*sn*-glycero-3-phosphoethanolamine) or POPC (1-palmitoyl-2-oleoyl-*sn*-glycero-3-phosphocholine) and 2,5-ATH or 2,6-BATH were dissolved in 10 mL of dichloromethane, leading to clear solutions. From these stock solutions, volumes were taken and mixed in a different container, providing a lipid/additive molar ratio of 100:1. The mixed solutions were clearly homogeneous. The solvent was initially removed under a gentle air stream, and residual traces were removed with vacuum at room temperature for at least 30 min. For each dry homogeneous mixture, hydration was performed with 1.0 mL of a Britton-Robinson buffer[13] of chosen pH. No lipid degradation was observed upon different pH environments. Decomposition of phospholipids into the corresponding fatty acid and lysolipid can produce uncommon (double-bilayer) phases.[14] The calculated pK_a values of the OH groups attached to the aromatic rings are within the range from 9.6 and 10.3.[15]

X-ray Scattering Measurements. SAXS (small angle X-rays scattering) measurements were carried out at beamlines A2 (HASYLAB) and A02 (LNLS), λ = 0.15 nm, using bidimensional MarCCD detectors (LNLS acknowledges FAPESP project multiuser 2004/09447-9). The samples were placed in glass capillaries of 1 mm diameter inserted into metal blocks with controlled temperature.

The samples were prepared at least 24 h prior to the measurements. In both instruments they were left to rest at each desired temperature at least 5 min prior to data acquisition. The 2D data were circularly integrated using fit2D,[16] producing the equivalent of a high-resolution 1D pattern.

WAXS (wide angle X-rays scattering) measurements of the samples at room temperature did not show any significant diffraction profile, and further measurements at higher temperatures were therefore not carried out. Such results were expected for POPC, which does not show a gel phase at positive temperatures. For POPE, our studies started just above the temperature of the gel to liquid-crystalline phase transition ($L_\beta \rightarrow L_\alpha$ at 25 °C),[17] and the ATHs added to the lipid matrix did induce changes in the structure formed by this lipid at room temperature.

RESULTS AND DISCUSSION

We are interested in the influence of such ATHs on the local structure of cell membranes. However, we focused on their mixtures with pure lipids, to avoid the interaction with other compounds present on cell membranes, e.g., proteins and glycolipids, due to the intrinsic difficulty to isolate each contribution. Moreover, the interaction of ATHs with phospholipids at different pH values highlights the effect of charge/polarity on the morphology of the bilayer. For that, lipids with different overall charges on the headgroup, but identical alkyl chains, have been selected, namely POPE and POPC.

POPE/2,6-BATH System. X-ray diffraction from mixtures of POPE/2,6-BATH, molar ratio 100:1 at different temperatures and pH values, showed the contribution of 2,6-BATH to the self-assembled lipid structure. Pure hydrated POPE forms a lamellar gel phase at low temperatures, turning L_α at 25 °C and hexagonal above 71 °C,[17] via a small two-phase-coexistence region, representing a thermally driven increase on the surface curvature. Our preparations showed a far more complex behavior, with different structures upon dependence of pH, additional to multiphases spanning over a very wide temperature range.

At pH 4, heating from room temperature, rich scattering patterns allowed us to identify a lamellar structure with peaks of high intensity, additionally to two cubic phases (Figure 1).

The indexation of the lower intensity peaks lead to two cubic structures $P4_332$ (Q^{212}) and $Im3m$ (Q^{229}), the latter also known as Plumber's nightmare and commonly represented by a Schwartz's P-surface. The lamellar phase is observed up to 75 °C with a continuous minor decrease in the lattice parameter, indicating dehydration accompanied by increasing alkyl chain fluidity, as observed in many phospholipids, e.g., ref 18. More interesting is the lattice variation of the cubic phases, which expand until the

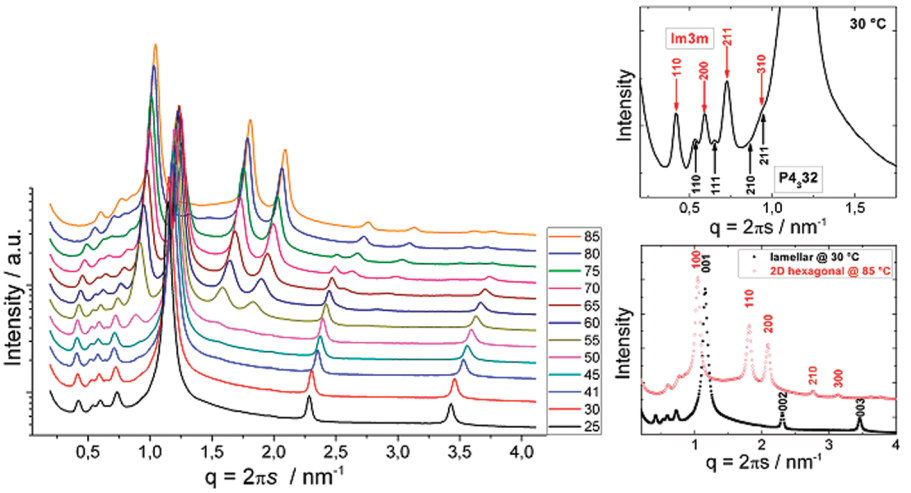

Figure 1. Left: Integrated experimental scattering intensities of a heating sequence for the sample containing POPE/2,6-BATH, 100:1, at pH 4. Right: Selected patterns illustrating the Miller indexes attributed to the peaks leading to the structures identified.

proximity of occurrence of a hexagonal phase, when they decrease nonlinearly (Figure 2).

It is worth noting two aspects: (a) both cubic phases followed similar thermal evolution of their lattice sizes up to 75 °C, when the $P4_332$ vanishes. After that, the *Im*3*m* became even more thermally sensitive. (b) after its onset, the hexagonal phase also decreased in lattice size upon heating, but with a smaller thermal sensitivity than the coexisting cubic ones (Figure 2).

Similar preparations, but at pH 8 and 9, lead to rather different behavior. At room temperature, under such conditions we observed two lamellar phases and a single cubic, *Im*3*m*, in sharp contrast with the preparation in acidic medium. The temperature onset of the cubic $P4_332$ increased with higher pH values. Looking at the lamellar phases, the one with larger *d* is attributed to a stabilized gel phase. At pH 8 it is still identifiable at 45 °C, while at pH 9 only traces of its diffraction peaks can be seen at 35 °C.

In basic environment, above 45 °C, we again observed two cubic phases, however, with different thermal sensitivities. While at pH 4 the lattice parameter shows a maximum at 40 °C, for pH 8 and 9 it continuously increased from room temperature until the structures collapsed above 75 °C. In those cases we did not see the decrease in cubic lattice size prior to the formation of the hexagonal phase. However, this hexagonal phase formed at similar temperatures and with similar lattice parameter as at pH 4. This is a strong suggestion that charge/polarity is the dominating contribution to the interaction between the headgroups, despite large differences in pH, inducing the cubic morphology of the bilayer surface. The thermal contribution at higher temperatures controls the structure formation. This means that 2,6-BATH headgroups are strongly polarized, or even hold an electrical charge (positive at pH 4), modifying drastically the balance of lipid headgroup interactions that occur in the pure lipid (POPE) system.

POPC/2,6-BATH System. The further investigation of charge/polarity in lipid/2,6-BATH interaction led to the POPC/2,6-BATH system. Pure hydrated POPC has a phase transition from gel to lamellar liquid-crystalline at −4 °C and does not spontaneously form a hexagonal phase.[17a] The POPC/2,6-BATH system, composed of a lipid with smaller charge/polarity, forms essentially the same structures as for the single lipid at low temperatures, not being significantly affected by the incorporation of 2,6-BATH.

At all pHs we identify lamellar phases up to above 50 °C with only a minor decrease in the dimensions of the lattice parameter upon heating. The sample with pH 4, at 65 °C, shows a broad peak at $q = 0.84$ nm^{-1} above a strongly increased diffuse scattering, indicative of a disintegrating lamellar phase, most likely into micelles. At basic condition, pH 8, it shows lamellar structures, characterized by broad and intense diffraction peaks (6.69 nm at 53 °C) (Figure 3).

Heating all samples induces slight broadening of the peaks from lamellae and introduces contributions with very low intensities, making an assignment to a specific structure not possible. This effect is far more visible in the samples at basic conditions. It indicates that increasing pH enhances the interaction between the alkyl chains, stabilizing the highly packed core of the bilayer. Simultaneously, we have less repulsive interaction between the headgroups on the bilayer surface.

The outcome of the investigation with these systems shows a rather less significant effect of 2,6-BATH on POPC than on the charged lipid POPE. Most strikingly, no cubic phases are formed with POPC in all temperatures and pH values studied. It indicates that charge/polarity interaction is an important contribution to the morphology of these systems in the temperature range between ca. 30 and 70 °C.

POPE/2,5-ATH System. Another single chained hydroquinone, 2,5-ATH (Scheme 2), has been mixed with POPE, enabling a direct comparison of the effect of multiple alkylthio chains of the additive on the interaction with this lipid. The mixture did not change the morphology found for pure lipid self-assembly, consequently also not inducing the formation of different (cubic) phases. However, it is worth noting that the patterns, both at pH 4 and 8, show three very well-defined diffraction orders and that at pH 4 the transition $L_\alpha \rightarrow$ Hex is shifted to a lower temperature, with the Hex phase already clearly seen at 63 °C (d_{100} = 6.31 nm) coexisting with L_α d = 5.17 nm (Figure 4). Moreover, at pH 8 the L_α phase shows a larger lattice parameter than at pH 4 for the equivalent temperature.

It is very interesting to observe that despite both additives 2,5-ATH and 2,6-BATH differ mainly by one alkylthio chain, their influence on the POPE matrix is so different. It indicates

dx.doi.org/10.1021/la200768x |*Langmuir* 2011, 27, 8257–8262

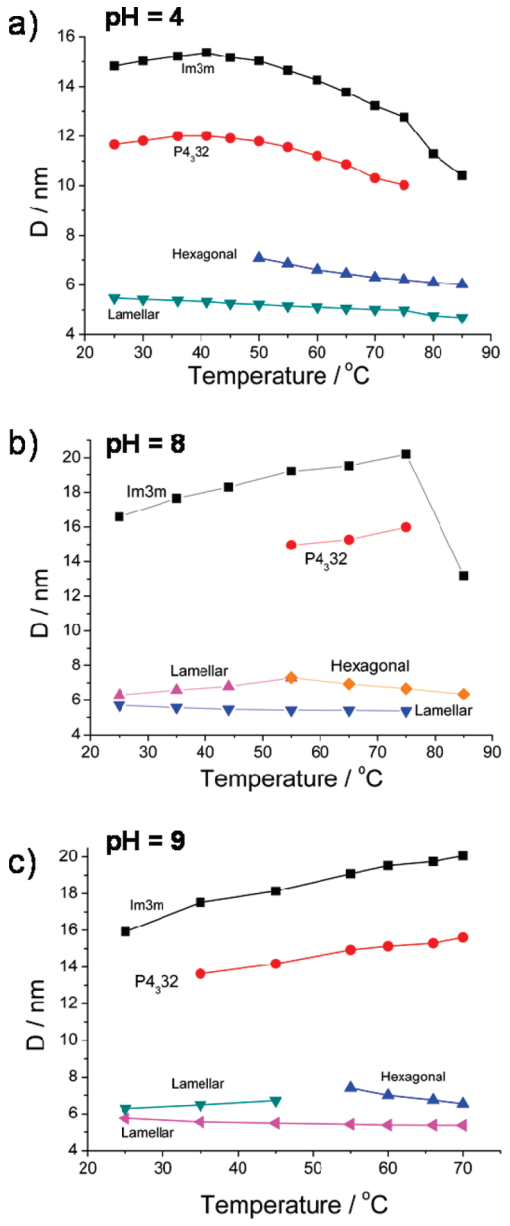

Figure 2. (a) Thermal evolution of the spacings of different phases formed by the POPE/2,6-BATH system at pH 4. Note the change upon the cubic phase near the hexagonal phase formation. Similar evolution for POPE/2,6-BATH at pH 8 (b) and pH 9 (c).

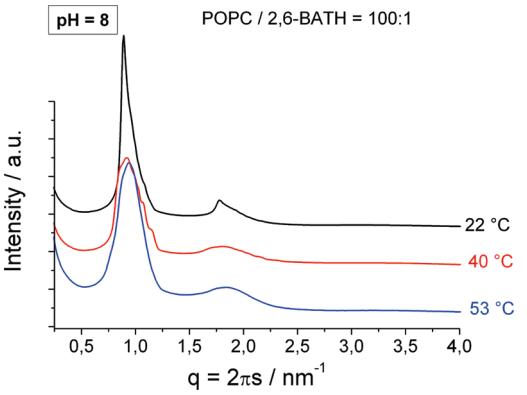

Figure 3. Heating sequence of scattering patterns of a mixture of POPC/2,6-BATH, 100:1, at pH 8. Note decreasing intensity and broadening of patterns taken at temperatures above 25 °C.

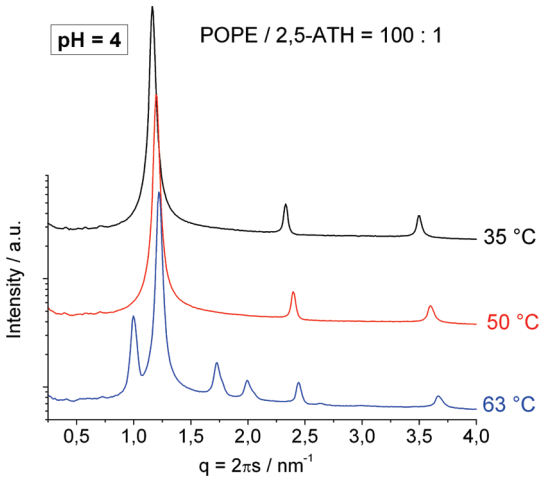

Figure 4. Heating sequence of scattering patterns of a mixture of POPE/2,5-ATH, 100:1, at pH 4. Note that the pattern containing lamellar and hexagonal phases was taken at a temperature well below the $L_\alpha \rightarrow$ Hex phase transition.

that the anchoring of the hydrophobic tails of the additive into the POPE bilayer also plays a decisive role in the morphology of the units forming the observed structure, additionally to the contribution of the charge/polarity of the additive.

The POPE/2,6-BATH mixtures at molar ratio 100:1 show a multidomain system, one with characteristics of hydrated POPE, with lamellae turning hexagonal upon heating, and another forming cubic phases, particular to the mixture, i.e., induced by the interaction of 2,6-BATH with the lipid. The cubic phases observed in these conditions have been identified as $P4_332$ and *Im*3*m*. These phases are particularly interesting because of their curvature. The $P4_332$ is an inverted cubic phase characterized by a network of rods embedding a matrix of micelles[19] (Figure 5a). Recently, new models for the *Im*3*m* phase have been proposed. One is a triple network structure[20] and another consists of two aggregation modes: a network of rods and spherical shells involving sheet-like units, resembling a closed lamellar structure[21] (Figure 5b).

Under acidic conditions, the cubic structures initially expand slightly upon heating. After 40 °C, they decrease, but with a larger rate of change (Figure 2). We associate this stronger variation with dehydration of the structure, inevitably packing the mesogenic units closer to each other. Considering the chemical formulae of the ATHs and lipid molecules forming our mixtures, one can see that protonation of the headgroups increases their overall charge and therefore the repulsion between neighbor molecules; see Scheme 2. To keep the hydrophobic core, the surface curvature decreases slightly. This mainly signifies that the change in the mesogenic unit curvature is the driving force allowing for the change in size of the structure. In parallel, one expects an increasing fluidization of the hydrophobic chains.

Changing to basic condition, the POPE/2,6-BATH system shows a structural behavior far more complex. The lamellar and hexagonal phases observed show significant changes from the behavior of the hydrated pure lipid and to the formation of the *Im*3*m* cubic phase. The diffraction patterns of these mixtures at

dx.doi.org/10.1021/la200768x |*Langmuir* 2011, 27, 8257–8262

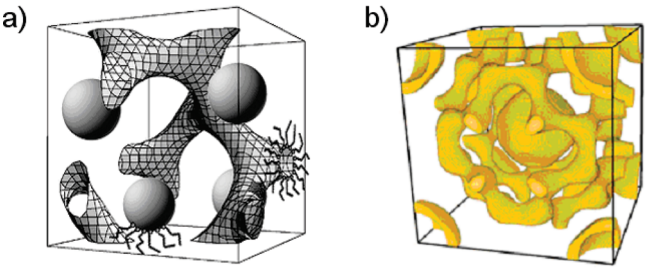

Figure 5. (a) Tentative representation of the cubic phase $P4_332$ (Q^{212}). (b) Region of high electron density consisting of molecular cores in a unit cell of the $Im3m$ (Q^{229}) phase of 1,2-bis(4′-*n*-alkoxybenzoyl)-hydrazine (BABH(*n*)) (reprinted from ref 21a with permission. Copyright 2009 Elsevier B.V.).

ambient temperature are quite striking, clearly showing the formation of two lamellar and one cubic phases, with the signals from the lamellar phases being much stronger (Figures 1 and 2).

We observed two lamellar phases occurring simultaneously in each basic system. It can be seen in Figure 2b,c that the one with larger *d* is less heat resistant and vanishes at different temperatures with varying pH, i.e., above 55 °C at pH 8 and above 45 °C at pH 9. At the higher pH value a stronger charge/polarity screening takes place favoring the structure with smaller lattice parameter. Note that the larger lattice, ∼6.3 nm, is closer to the lamellar gel than fluid lamellar phase

It has been observed elsewhere that lipid/additive mixtures form expanded lamellar phases with lattice parameter similar to the hexagonal structure upon a temperature-driven phase transition.[18] Here, the charge/polarity plays the important role in determining the curvature on the lipid matrix surface as well as the dimensions of the structure formed. The repulsion among the POPE and 2,6-BATH headgroups decreases considerably compared to that at pH 4 to such an extent that the formation of micelles becomes feasible. The formation of a network can more easily accommodate such interactions by adjusting the lateral separation of the molecules and therefore the rod diameter. From the perspective of the hydrophobic chains, the major effect is to increase thermal motion, but not considerably the bilayer thickness. The effects of headgroup overall polarization in nonionic surfactants and their induction of microdomains on lipids are illustrated in ref 22. Hydration level can also lead to very high local curvature.[23]

The coexistence of units with different surface curvature is indicative of a nonhomogeneous distribution of the 2,6-BATH molecules, being higher in the smaller micelles and lower in the planar surface of the lamellae. The local concentration of 2,6-BATH causes different charge/polarity on the bilayer surface, allowing for a different local curvature over it. This, if tuned to desirable values, has the potential for interaction with other alien molecules and shall be interesting in further drug delivery investigations upon selective interactions on the cell surface.

It is tempting to speculate on the consequences of coexistence of different nonlamellar phases in real cells. If not compensated by other components of the cell membrane, the structures induced by ATHs certainly would have dramatic effects on the cell function. The formation of units with high curvature could lead to disruption of the membrane, causing leakage of the interior content. However, one should have in mind that the ATHs studied here resemble CoQ, which is accepted to lie in the hydrophobic core of the inner membrane of mitochondria, where cistae (invaginations) intrinsically presenting high curvature are a common feature.[24] On the other hand, the rod network formation with variable diameter could, if locally stable, allow for selective trans membrane transport. Size and interaction with the ATHs would determine which substances could be transported.

CONCLUSION

The mixtures of lipid/ATHs reported in this study covered a wide range of interactions. In all cases we observed the formation of phases, similar to the behavior of the pure hydrated lipids. For POPC, we observe lamellar phases with almost no influence of 2,6-BATH, while for POPE we observe a strong influence. Two lamellar phases are seen at room temperature, and the onset of the hexagonal is shifted to lower temperature, in addition to cubic structures. These cubic phases are the result of interactions between the POPE and 2,6-BATH.

The variation of pH values clearly illustrated differences in the overall interactions, producing cubic structures with different relative stabilities. Under acidic conditions POPE/2,6-BATH forms two coexisting cubic phases, $Im3m$ and $P4_332$, structures containing different aggregates, consistent with rods and spherical units, while under basic conditions the $P4_332$ cubic phase occurs at higher temperatures, and the thermal onset is bigger at higher pH. The 2,5-ATH is not able to induce the formation of cubic phases in POPE in either acidic (pH 4) or basic (pH 8 and 9) environments.

For the polar lipid POPE, the charge/polarity of the ATHs affect the lipid matrix depending on the pH, inducing the formation of structures with high curvature, such as micelles; this is more effective at pH 4 than under basic conditions. In parallel, for the zwitterionic POPC charge/polarity effects is almost negligible.

The number of alkylthio chains attached to the ring on the hydroquinone, imbedded on the lipid matrix, also has a dramatic effect. 2,5-ATH, with one chain only, decreases the temperature of transition from lamellar to hexagonal phase in POPE, but does not induce cubic structures comparative to two cubic phases induced by the 2,6-BATH, with two alkylthio chains.

AUTHOR INFORMATION

Corresponding Author

*E-mail: sergio.funari@desy.de.

ACKNOWLEDGMENT

We thank Drs. J. A. Brum, I. Torriani, H. Westfahl Jr., and R. A. Martinez for their competence and support prior to and during the measurements at LNLS.

REFERENCES

(1) Thomson, R. H. *Naturally Occurring Quinones IV*; Blackie Academic & Professional: London, 1997. Hargreaves, R. H. J.; Hartley, J. A.; Butler, J. *Front. Biosci.* **2000**, *5*, 172.Morton, R. A. *Biochemistry of Quinones*: Academic Press: London, 1965. Patai, S.; Rappoport, Z. *The Chemistry of the Functional Groups in The Chemistry of the Quinonoid Compounds*; John Wiley & Sons: New York, 1988. Oostveen, E. A.; Speckamp, W. N. *Tetrahedron* **1987**, *43*, 255. Colucci, M. A.; Moody, C. J.; Couch, G. D. *Org. Biomol. Chem.* **2008**, *6*, 637.

(2) Koyama, J. *Recent Pat. Anti-infect. Drug Discovery* **2006**, *1*, 113. Monks, T. J.; Hanzlik, R. P.; Cohen, G. M.; Ross, D.; Graham, D. G. *Toxicol. Appl. Pharmacol.* **1992**, *112*, 2. Koichi, M.; Kyoko, T.; Takeo, K.;

Hiroteru, S. *Chem. Pharm. Bull.* **1987**, *35*, 1270. Staisiuk, M.; Kozubeck, A. *Cell. Mol. Life Sci.* **2010**, *67*, 841.
(3) Luzzati, V. In *Biological Membranes*; Chapman, D., Ed.; Academic Press: London, 1968.
(4) Rappolt, M.; Hickel, A.; Bringezu, F.; Lohner, K. *Biophys. J.* **2003**, *84*, 3111. Rappolt, M. *Biophys. J.* **2003**, *84*, 3111. Rappolt, M.; Vidal, M. F.; Kriechbaum, M.; Steinhart, M.; Amenitsch, H.; Bernstorff, S.; Laggner, P. *Eur. Biophys. J.* **2003**, *31*, 575.
(5) Siegel, D. P. *Biophys. J.* **1986**, *49*, 1155. Siegel, D. P. *Biophys. J.* **1994**, *66*, 402. Siegel, D. P. *Biophys. J.* **1999**, *76*, 291.
(6) Koynova, R.; Caffrey, M. *Chem. Phys. Lipids* **1994**, *69*, 1.
(7) Tenchov, B.; Koynova, R.; Rapp, G. *Biophys. J.* **1998**, *75*, 853. Rapp, G.; Koynova, R.; Tenchov, B. *Biophys. J.* **1998**, *74*, A27.
(8) Uhrikova, D.; Pullmannova, P.; Bastos, M.; Funari, S. S.; Teixeira, J. *Gen. Physiol. Biophys.* **2009**, *28*, 146.
(9) Koynova, R. D.; Tenchov, B. G. *Biochim. Biophys. Acta* **1983**, *727*, 351.
(10) Wiese, W.; Harbich, W.; Helfrich, W. *J. Phys. Condens. Matter* **1992**, *4*, 1647.
(11) Siegel, D. P. *Biophys. J.* **2008**, *94*, 3987.
(12) Mares, T.; Daniel, M.; Perutkova, S.; Perne, A.; Dolinar, G.; Iglic, A.; Rappolt, M.; Kralj-Iglic, V. *J. Phys. Chem.* **2008**, *112*, 16575.
(13) Britton, H. T. K.; Robinson, R. A. *J. Chem. Soc* **1931**, 1456. Mongay Fernández, C.; Cerdá Martin, V. *Talanta* **1977**, *24*, 747.
(14) Funari, S. S.; Rapp, G.; Richter, F. *Quim. Nova* **2009**, *3*, 908.
(15) http://aceorganic.pearsoncmq.com/epoch-plugin/public/pKa.jsp, accessed on 21st March 2010.
(16) http://www.esrf.fr/computing/scientific/FIT2D, accessed on 14th April 2010.
(17) Wang, X. Y; Quinn, P. *Biochim. Biophys. Acta* **2002**, *1564*, 66. (a) Marsh, D. *CRC Handbook of Lipid Bilayers*; CRC Press: Boca Raton, FL, 1990.
(18) Prades, J.; Funari, S. S.; Escribá, P. V.; Barceló, F. *J. Lipid Res.* **2003**, *44*, 1720.
(19) Esposito, E.; Eblovi, N.; Rasi, S.; Drechsler, M.; G. M. Di Gregorio, Menegatti, E.; Cortesi, R. *AAPS PharmSci.* **2003**, *5* (4), Article 30.
(20) Zeng, X. B.; Cseh, L.; Mehl, G. H.; Ungar, G. *J. Mater. Chem.* **2008**, *18*, 2953.
(21) (a) Saito, K.; Nakamoto, T.; Sorai, M.; Yao, H.; Ema, K.; Takekoshi, K.; Kutsumizu, S. *Chem. Phys. Lett.* **2009**, *469*, 157. (b) Ozawa, K.; Yamamura, Y.; Yasukuda, S.; Mori, H.; Kutsumizu, S.; Saito, K. *J. Phys Chem. B Lett.* **2008**, *112*, 12179.
(22) Funari, S. S.; Rapp, G. *Proc. Nat. Acad. Sci. U. S. A.* **1999**, *96*, 7756. Funari, S. S.; Nuscher, B.; Rapp, G.; Beyer, K. *Proc. Nat. Acad. Sci. U. S. A.* **2001**, *98*, 8938.
(23) Yang, L.; Huang, H. W. *Science* **2002**, *297*, 1877.
(24) Voegt, D.; Voegt, J. G. *Biochemistry*, 2nd ed.; John Wiley & Sons, Inc: New York, 1994; Chapter 20.

NOTE ADDED AFTER ASAP PUBLICATION

This paper was published on the Web on June 1, 2011. The title of Scheme 2 has been updated. The corrected version was reposted on June 6, 2011.